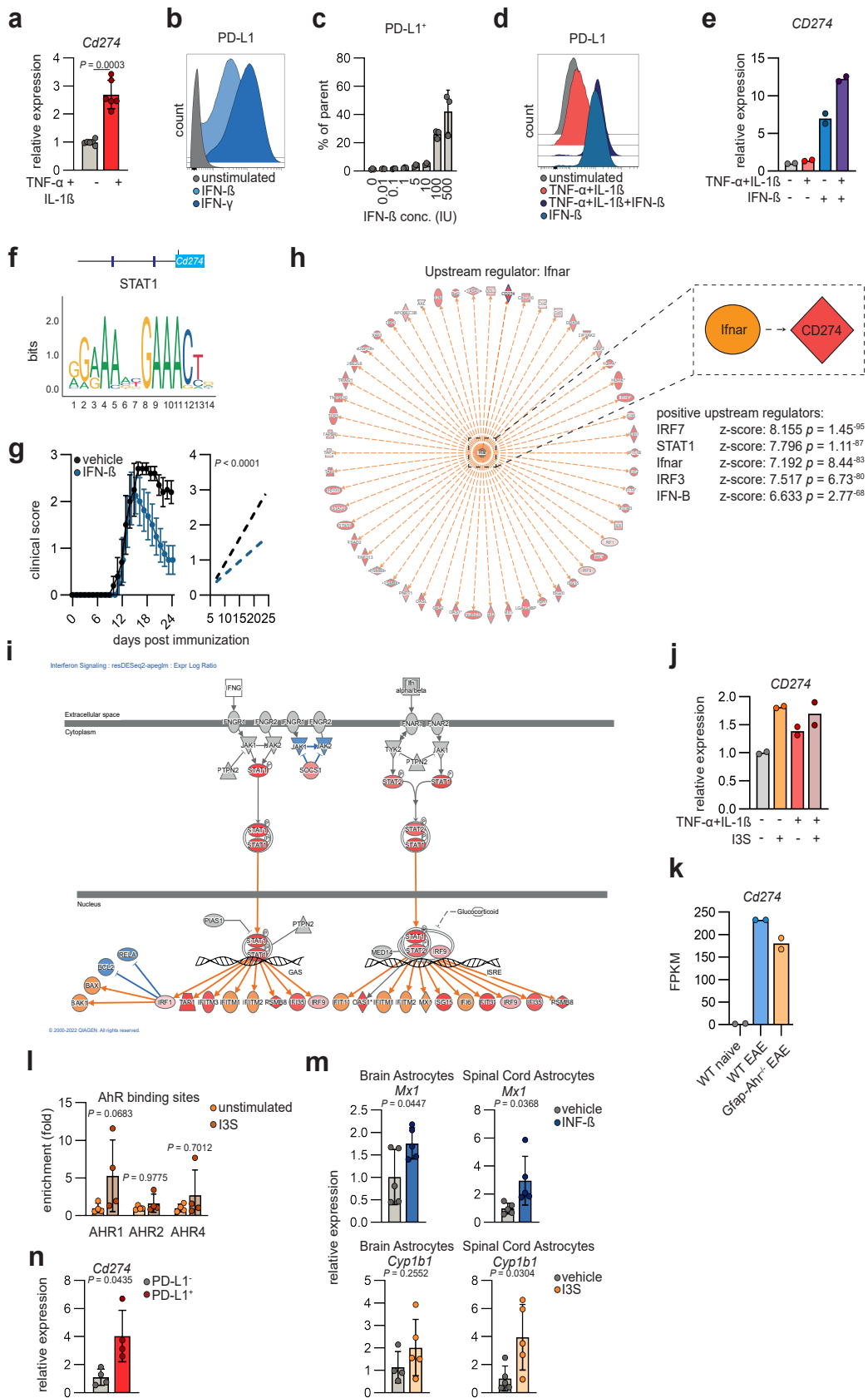
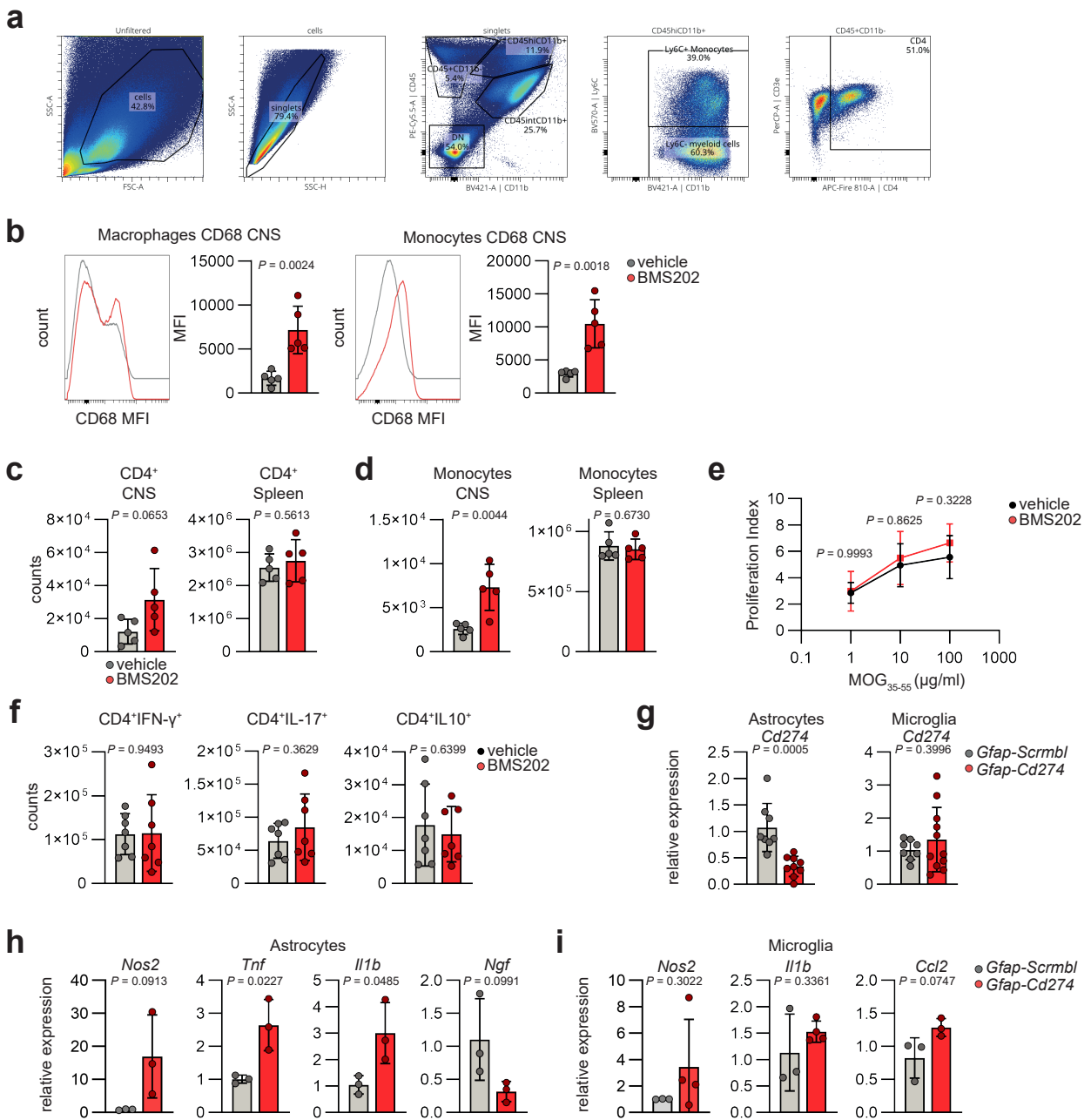


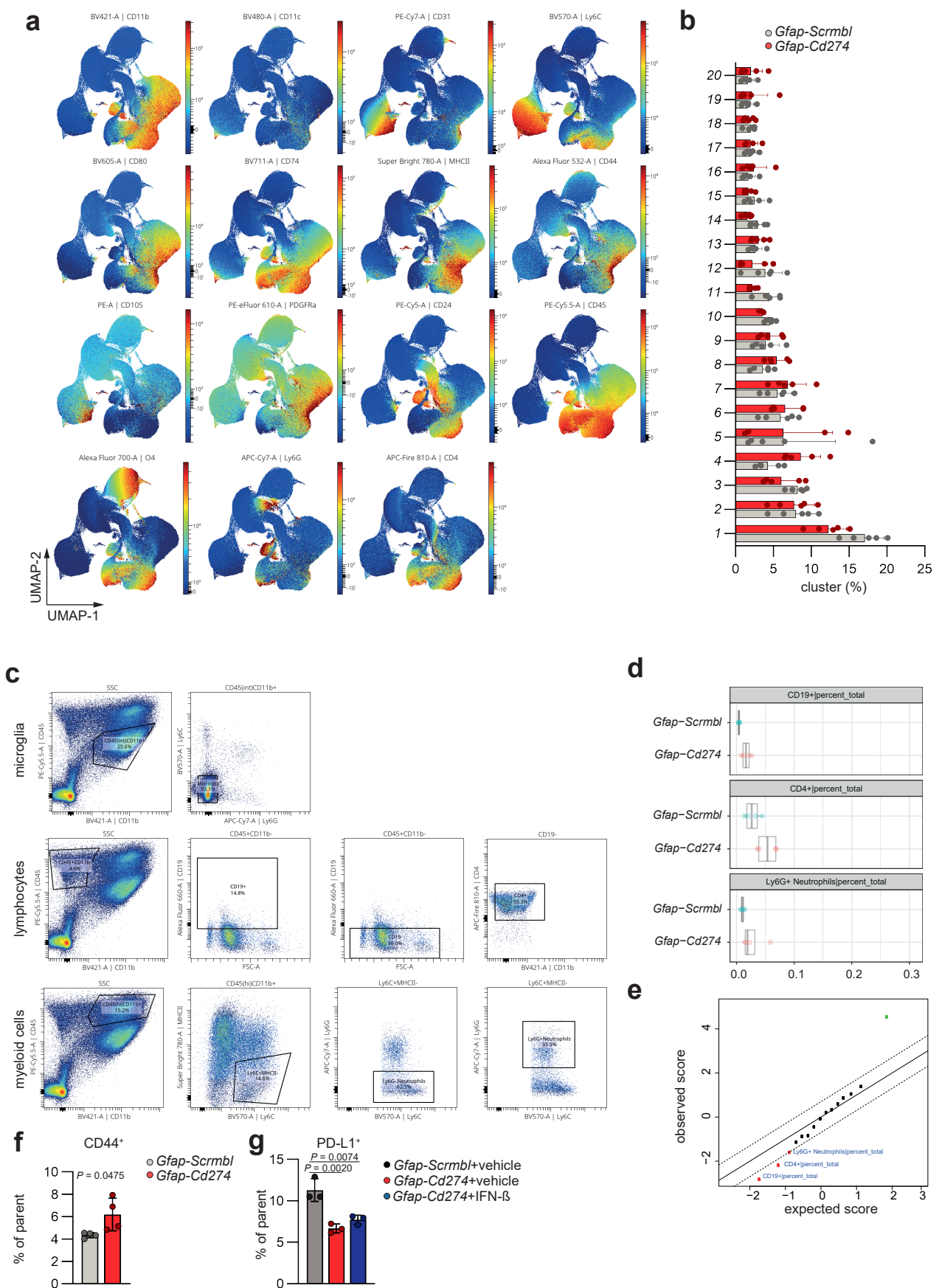
Supplementary Figure 1. Astrocytic expression of PD-L1 in the context of CNS inflammation. **a**, relative PD-L1 expression (% of parent) and absolute counts by astrocytes ($n = 11$), monocytes ($n = 7$), and microglia ($n = 12$) in the inflamed CNS quantified by flow cytometry. **b**, immunohistochemical staining of PD-L1⁺ astrocytes (GFAP⁺; left) and microglia (Iba1⁺; right) in normal appearing white matter (NAWM) from MS patients. 30 μ m scale bar. **c**, sorting strategy for astrocytes from CNS and expression of astrocyte markers *Gfap*, *Aqp4*, *Aldh11l1*, *Gja1*, and *S100b* by sorted astrocytes ($n = 4$) and non-astrocytes ($n = 10$) quantified by RT-qPCR. **d**, normalized relative expression of genes in PD-L1⁺ and PD-L1⁻ EAE astrocytes. $n = 3/10$ PD-L1⁺, $n = 3/10$ PD-L1⁻. **e**, tSNE plot (upper) and Visium spatial expression (lower) of Cd274 expression in astrocyte subclusters following peripheral LPS- or vehicle (CONT)-injection obtained from Hasel et al. 86. **f**, mRNA expression of metalloproteases Adam10, Adam17, Mmp9, and Mmp13 in sorted astrocytes at the naive, peak and recovery stage of EAE. One-way ANOVA with Tukey's multiple comparisons test in **(a)**, unpaired t-test with two-stage step-up FDR control in **(c, d)**. Exact P-values are provided in the figure. Data are shown as mean \pm SD.



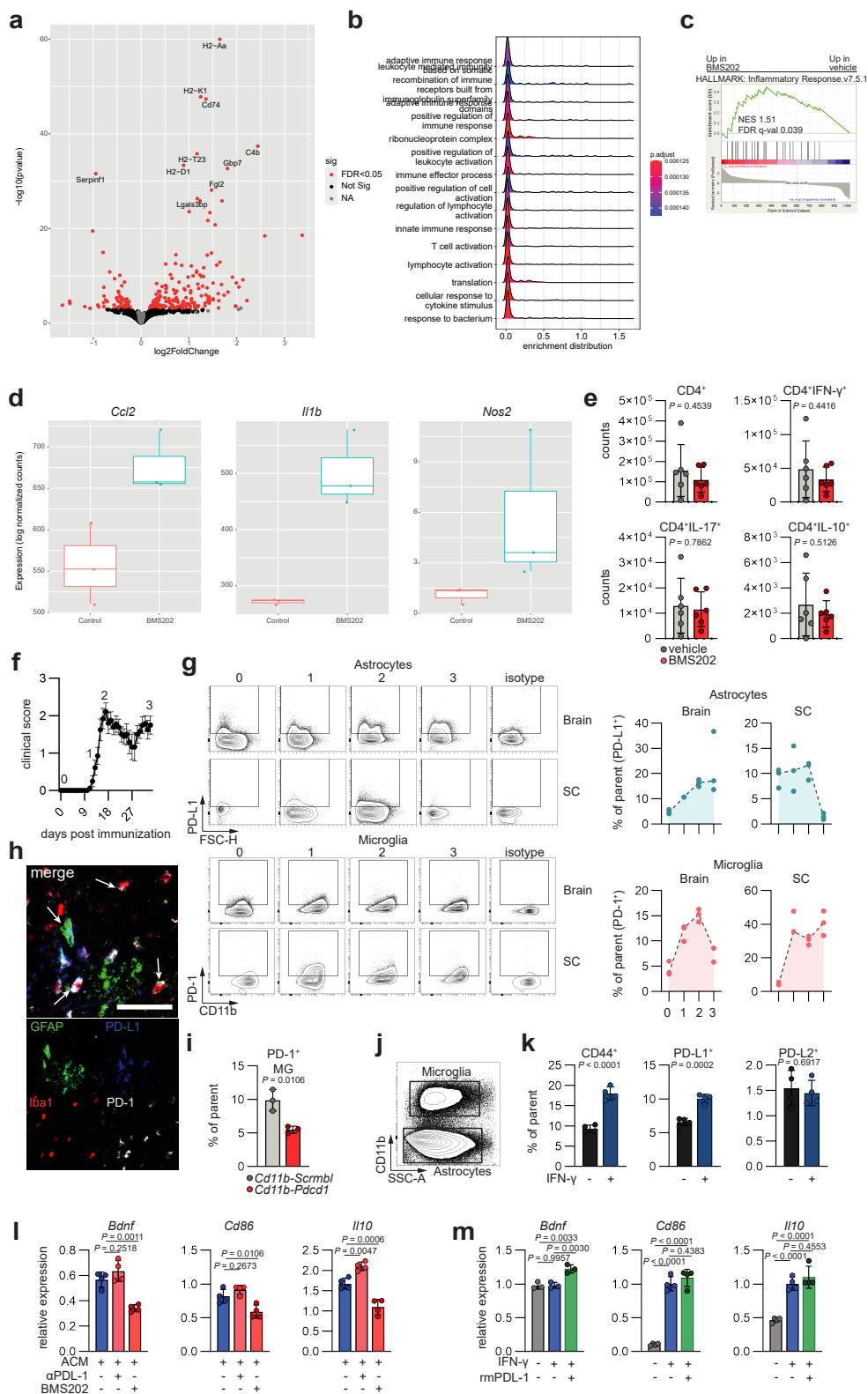
Supplementary Figure 2. Transcriptional control of *Cd274* in astrocytes. **a**, *Cd274* expression by primary mouse astrocytes following stimulation with TNF- α and IL-1 β or vehicle. $n = 5$ per group. **b**, representative scatterplots (entire group concatenated) of PD-L1 expression by primary mouse astrocytes following stimulation with IFN- β , IFN- γ , or vehicle. $n = 3$ per group. **c**, flow cytometric quantification (% of parent) of PD-L1 expression by primary mouse astrocytes following stimulation with different concentrations of IFN- β . $n = 3$ per group. **d**, representative scatterplots (entire group concatenated) of PD-L1 expression by human astrocytes following stimulation with TNF- α , IL-1 β , and IFN- β . $n = 3$ per group. **e**, *CD274* expression by human astrocytes in response to TNF- α and IL-1 β \pm IFN- β . $n = 2$ per group. **f**, predicted STAT1-binding sites in the *Cd274* promoter by JASPAR 34. **g**, EAE development in mice intranasally treated with vehicle or IFN- β starting at day 7 post immunization. $n = 5$ per group. Experiment repeated twice. **h**, Ingenuity Pathway Analysis of the upstream regulatory network in astrocytes derived from EAE mice that received intranasal IFN- β administration. Upregulation in comparison to vehicle treated mice is indicated by red color. **i**, interferon signaling network in astrocytes derived from EAE mice that received intranasal IFN- β administration. Upregulation in comparison to vehicle treated mice is indicated by red color, downregulation by blue color. **j**, *CD274* expression by human astrocytes in response to TNF- α and IL-1 β \pm I3S. $n = 2$ per group. **k**, Fragments Per Kilobase Million (FPKM) values of sorted astrocytes from WT, WT EAE, and GFAP^{Cre} AhR^{fl/fl} EAE mice. $n = 2$ per group. **l**, ChIP-qPCR analysis of AhR recruitment to the *Cd274* promoter following stimulation with I3S or vehicle, $n = 4$ per group. **m**, *Mx1* (IFN-signaling control) and *Cyp1b1* (AhR-signaling control) expression by astrocytes obtained from EAE mice intranasally treated with IFN- β or I3S. $n = 5$ per group. **n**, *Cd274* expression by PD-L1+ and PD-L1- sorted astrocytes. $n = 4$ per group. Unpaired t-test (two-sided) in (**a**, **m**, **n**), Linear regression starting day 7 p.i. in (**g**), One-way ANOVA with Dunnett's multiple comparisons test in (**f**), Two-way ANOVA with Sidak's multiple comparisons test in (**l**). Exact P-values are provided in the figure. Data are shown as mean \pm SEM in (**g**). Data are shown as mean \pm SD if not indicated otherwise.



Supplementary Figure 3. Astrocyte-derived PD-L1 attenuates neuroinflammation. **a**, gating strategy used identify Ly6C⁺ monocytes and CD4⁺ T cells in the CNS (and spleen). **b**, representative scatter plots and median-fluorescence intensity (MFI) quantification of CD68 expression by macrophages and monocytes in the CNS of vehicle or BMS202-treated mice. $n = 5$ per group. **c**, counts of CD4⁺ T cells in the CNS and spleen of BMS202 or vehicle-treated mice. $n = 5$ per group. **d**, counts of Ly6C⁺ monocytes in the CNS and spleen of BMS202 or vehicle-treated mice. $n = 5$ per group. **e**, proliferation index of splenic CD4⁺ T cells obtained from BMS202 or vehicle-treated mice that were challenged with varying concentrations of MOG₃₅₋₅₅ in vitro. $n = 9$ per group. **f**, counts of TH1 (CD4⁺CD11b⁺CD4⁺IFN- γ ⁺), TH17 (CD4⁺CD11b⁺CD4⁺IL-17⁺), and regulatory IL-10⁺CD4⁺ T cells in spleens of vehicle or BMS202 treated mice. $n = 7$ per group. **g**, Cd274 expression in FACS-sorted astrocytes and microglia from Gfap-Scrmbl ($n = 8$) and Gfap-Cd274 EAE mice ($n = 9/11$). **h**, mRNA expression of *Nos2*, *Tnf*, *Il1b*, *Ngf* by astrocytes (Gfap-Scrmbl $n = 3$; Gfap-Cd274 $n = 3$) (**h**) and *Nos2*, *Il1b*, *Ccl2* by microglia (Gfap-Scrmbl $n = 3$; Gfap-Cd274 $n = 3/4$) (**i**) from Gfap-Scrmbl and Gfap-Cd274 EAE mice. Two-way ANOVA with Sidak's multiple comparisons test in (**e**), unpaired t-test (two-sided) if not indicated otherwise. Exact P-values are provided in the figure. Data are shown as mean \pm SD in if not indicated otherwise.



Supplementary Figure 4. Astrocyte-derived PD-L1 regulates CNS inflammation. **a**, UMAP plots of CNS cells analyzed by high-dimensional flow cytometry in *Gfap-Scrmbl* ($n = 5$) and *Gfap-Cd274* ($n = 5$) mice. The color represents the intensity of the respective surface marker (red indicates high expression, blue indicates low expression). **b**, relative abundance (% of singlets) of FlowSOM clusters in the CNS of *Gfap-Scrmbl* ($n = 5$) and *Gfap-Cd274* ($n = 5$) mice analyzed by high-dimensional flow cytometry. **c**, representative gating strategy for microglia, lymphocytes, myeloid cells and their respective subsets. **d**, SAM (Statistical Analysis of Microarray) 78 boxplots and SAM-plot (**e**) of cell population abundances in the CNS that were significantly different between *Gfap-Scrmbl* and *Gfap-Cd274* mice. $n = 4$ per group. **f**, CD44 expression (% of parent) by microglia in *Gfap-Scrmbl* and *Gfap-Cd274* mice during EAE. $n = 4$ per group. **g**, flow cytometric quantification of PD-L1 expression by astrocytes in *Gfap-Scrmbl* and *Gfap-Cd274* mice that were intranasally treated with vehicle or IFN- β . $n = 3$ per group. One-way ANOVA with Tukey's multiple comparisons test in (**g**), unpaired t-test if not indicated otherwise. Data are shown as mean \pm SD if not indicated otherwise. Data are shown as mean with the 25th and 75th percentiles in (**d**).



Supplementary Figure 5. PD-L1 / PD-1 signaling modulates glial responses during chronic neuroinflammation. a, volcano plot of genes differentially regulated in microglia derived from NOD/ShiLtJ treated with BMS202 or vehicle during the progressive phase of EAE. **b**, pathway enrichment and GSEA (**c**) of astrocytic gene expression from NOD/ShiLtJ mice treated with vehicle or BMS202. $n = 3$ per group. **d**, log normalized counts of *Ccl2*, *Il1b*, and *Nos2* expressed by microglia in NOD/ShiLtJ mice treated with vehicle or BMS202. $n = 3$ per group. **e**, counts of TH1 ($CD45^+CD11b^+CD4^+IFN-\gamma^+$), TH17 ($CD45^+CD11b^+CD4^+IL-17^+$), and regulatory $IL-10^+CD4^+$ T cells in the CNS of vehicle or BMS202 treated NOD/ShiLtJ mice. $n = 6$ per group. **f**, EAE development and timepoints indicated for the flow cytometric analysis of PD-L1 and PD-1 expression by glial cells. $n = 20$. **g**, representative scatterplots and quantification of PD-L1 expression by astrocytes, as well as PD-1 expression by microglia in the brain and spinal cord during EAE at the timepoints indicated in (**f**). $n = 3$ per timepoint and group. **h**, immunostaining of PD-L1⁺ astrocytes and PD-1⁺ microglia in brains of EAE mice. Data shown are representative of $n = 12$ fields from three distinct EAE brains. scale bar 50 μm . **i**, expression of microglial PD-1 expression in *Cd11b-Scrmbl* and *Cd11b-Pdcd1* mice during EAE, quantified by flow cytometry. $n = 3$ per group. **j**, representative scatterplot depicting the gating strategy used to separate microglia from astrocytes in the astrocyte-microglia co-culture. **k**, relative expression (% of parent) of the activation marker CD44 and the B7 family members PD-L1 and PD-L2 by primary mouse astrocytes stimulated with IFN- γ . $n = 4$ per group. **l**, RT-qPCR analysis of *Bdnf*, *Cd86*, and *Il10* by primary mouse microglia following blockade of soluble PD-L1 by BMS202 or α -PD-L1. $n = 4$ per group. **m**, RT-qPCR analysis of *Bdnf* ($n = 3$ per group), *Cd86* ($n = 4$ per group), and *Il10* ($n = 4$ per group) by IFN- γ -activated primary mouse microglia following treatment with rmPD-L1. Unpaired t-test in (**e**, **f**, **k**), One-way ANOVA with Tukey's multiple comparisons test in (**l**, **m**). Data are shown as mean \pm SEM in (**g**). Data are shown as mean \pm SD in if not indicated otherwise. Data are shown as mean with the 25th and 75th percentiles in (**d**).